Vibrational resonance of Ammonia molecule with doubly-singular position-dependent mass

Taiwo O. Roy-Layinde[1*], Kehinde A. Omoteso[1†], Babatunde A. Oyero[1†], John A. Laoye[1†] and Uchechukwu E. Vincent[2,3†]

[1*]Department of Physics, Olabisi Onabanjo University, Ago-Iwoye, P.M.B. 2002, Ogun State, Nigeria.
[2]Department of Physical Sciences, Redeemer's University, Ede, P.M.B. 230, Osun State, Nigeria.
[3]Department of Physics, Lancaster University, Lancaster, LA1 4YB, United Kingdom.

*Corresponding author(s). E-mail(s): roy-layinde.taiwo@oouagoiwoye.edu.ng;
Contributing authors: omotesokehinde@gmail.com; oyerobabs@gmail.com;
bidemi.laoye@oouagoiwoye.edu.ng; u.vincent@run.edu.ng;
†These authors contributed equally to this work.

Abstract

We examine vibrational resonance (VR) in a position-dependent mass (PDM) oscillator with doubly-singular mass distribution function describing the vibrational inversion mode of NH_3 molecule. The impacts of the PDM parameters (m_0, a, η) on VR was studied by computing the response amplitudes as functions of the amplitude of high-frequency component of the dual-frequency driving forces and the PDM parameters. We show for the first time that, beside the significant roles played by the parameters of the variable mass in inducing and controlling resonances similar to the forcing parameters, the variable mass parameters impacts on the resonance characteristics by leading the system from single resonance into double resonance.

Keywords: Vibration, Resonance, Ammonia Molecule, Position-dependent mass, Bi-harmonic driving

1 Introduction

Periodically forced oscillators can exhibit intriguing and nontrivial behaviors such as bifurcations, chaos and resonances. The term resonance was originally defined for forced oscillators, as the amplification of the system's response induced when the frequency of the external forcing matches the natural frequency of the system. Resonance has been redefined and generalized to describe all forms of amplifications induced by either internal or external influences. Nonlinear resonances are characterized by the enhancement of a low-frequency (LF) force by a high-frequency (HF) external force. Depending on the nature of external force acting on the system, the enhancement can appear in different forms, the prominent among them being stochastic resonance (SR) and vibrational resonance (VR) [1]. In SR, noise is added to the weak external signal in order to amplify the response of the output signal; while in VR the noise in SR is replaced by high-frequency (HF) periodic signal. VR is a very promising

mechanism for various applications including weak signal detection and attenuation of unwanted signal in systems [1, 2].

The last two decades has witnessed enormous growth in research works on VR in systems with different potentials [3–11]; some of which are adapted to theoretical and experimental studies on electrical and mechanical oscillators [12, 13], information [14] and image [15] processing, plasma [16], bubble [17], laser [18], neuron [19, 20], gyroscope [21, 22] and quantum systems [23, 24]. In these studies, majority of the systems are assumed to posses constant mass. However, some physical systems are known to posses variable mass which is due to alteration in the number of constituent particles as the system evolve with either time, position or velocity due to accretion or ablation processes [25]. The mass variation may arise from either monotonic decrease of mass through particle-ejection processes that are encountered in studies on rocket flight dynamics [26], motion of a falling meteorite [27], reel laying operation of marine cables [28], vertical collapsing tower [28] and tethering satellite dynamics [28], or monotonic increase of mass that characterizes particle-accreting systems such as formation of icebergs and raindrops [27], and accretion of planets and asteroids in the early solar system [29].

Systems with variable mass are non-conservative and their propagation dynamics is considerably different and more complicated in comparison to that of bodies with constant mass [30–33]. Various forms of variable mass have been shown to influence system's dynamics which could lead to several phenomena such as amplitude jump, hysteresis, nonlinear resonances, chaos, coexistence of attractors, multistability and resonance [34, 35]. For instance, a slowly varying deterministic time-dependent mass influences the severity of nonlinearity and birth of chaos in a rotor system [32]. Also, an interplay between position-dependent mass index and external signal produces remarkable phase transitions between regular motion and chaotic oscillation in a Duffing oscillator [34]. In quantum dots with position-dependent electron effective mass, the optical properties depends on the spatially varying effective mass [36]. The mass variation in these studies is usually defined as function of any of the system's generalized coordinates of either time, position or velocity. When the variable mass is explicitly dependent on position, the system is referred to as a position-dependent mass (PDM) system.

It is noteworthy that PDM systems have been well studied in material science and condensed matter physics in view of the potential applications of spatially varying mass, especially in understanding the physical properties of nanostructures and development of nanomaterials and nanotechnology from semiconductor theory [37], compositionally graded crystals [38], polarons [39], quantum liquids [40], nonlinear oscillators [41, 42], neutrino-mass puzzle [43], ^{3}Helium clusters [40, 44], quantum wells and dots [36], crystal lattices microstructures [45] and nuclear many-body problem [46]. In classical position-dependent mass systems, the modification of the equation of motion for bodies with constant mass to include a non-potential reactive force term which is a quadratic function of velocity derivable from Lagrangian and Hamiltonian mechanics has been emphasized [47].

Recently, Roy-Layinde *et al.*[33] studied VR in a Duffing-type PDM system with the mass distribution described by a *regular mass function* consisting of rest mass and a spatial nonlinearity index and developed a theoretical framework for dealing with VR in systems with position-dependent mass. Their results are remarkable as they showed that PDM parameters influence the VR phenomenon. The effective mass of a *regular mass-function* type is connected to the revival of wave packets in a position-dependent mass infinite well [48]. However, not all physical PDM systems posses mass that could be modeled by a *regular mass function*. For instance, the potential function for the vibrational inversion mode of NH_3 molecule, which we investigate in this paper, has been modeled based on density functional theory by a doubly-singular spatially varying mass-function [47, 49]. In view of the importance of varying mass on systems with different potential types and mass distribution functions encountered in various fields of sciences, particularly in condensed matter, molecular and optics physics [45, 47, 50], it is motivating to explore more closely the effects of PDM on VR in different systems for which varying mass exist. In this paper, we present the results of our numerical investigation of VR in a PDM oscillator whose mass is

described by a doubly-singular mass-function arising from the analysis of the inversion potential of NH_3 molecule. We explore the effect of the PDM parameters on the VR phenomenon with a view to control and initiate resonance through them. We report for the first time that, the variable mass parameters impacts on the resonance characteristics by leading the system from single vibrational resonance state into double vibrational resonance. Our results could provide more insight into the vibrational modes and spectroscopy of a wide range of systems enumerated above.

2 The Model

We consider the equation of motion for a biharmonically driven oscillator in a bistable potential $V(x)$, whose effective mass distribution $m(x)$ is a doubly-singular mass-function with a constant mass amplitude m_0. In general, bistable potentials can take the form of a trigonometric function [51, 52], hyperbolic function [53, 54] or polynomial function [49, 55, 56]. Here, we consider a simple bistable potential given by the following polynomial function:

$$V(x) = \frac{1}{2}m(x)\omega_0^2 x^2 + \frac{1}{4}\beta x^4, \tag{1}$$

where β is the coefficient of nonlinearity. $m(x)$ is taken to be a *doubly-singular mass-function* for NH_3 molecule. Aquino *et al.* [49] showed that the reduced mass μ of an inversion potential of NH_3 molecule can be written as a function of the inversion coordinate when the geometry is a regular triangular pyramid where nitrogen atom surrogates between both sides of the plane. In this arrangement, three hydrogen atoms each with mass m are placed at the vertices of the base and a nitrogen atom with mass M on the cusp, such that the coordinates of the nitrogen is $N(x, 0, 0)$, where x is the inversion coordinate. During the inversion, r is the N-H distance, so that r_0 is the N-H separation at the planar equilibrium geometry. The reduced mass μ is given by

$$\mu = \mu_0 + \frac{3mx^2}{r_0^2 - x^2}, \tag{2}$$

where $\mu_0 = \frac{3mM}{3m+M}$ is the reduced mass when the distance between each pair of masses m remains constant. By setting $r_0 = \frac{1}{a} > 0$ (expressed in distance unit), $\eta = 1 - \frac{3m}{\mu_0}$ (arbitrary negative dimensionless parameter), $\mu = m(x)$ and $\mu_0 = m_0 > 0$ (arbitrary constant expressed in unit of mass) in equation (2), we can write the reduced mass as

$$m(x) = \frac{m_0(1 - \eta a^2 x^2)}{1 - a^2 x^2}, \quad (a \geq 0, \eta < 0). \tag{3}$$

where η is the mass ratio and a is the separation coefficient. Equation (3) has two singularities at the points $x = \pm\frac{1}{a}$ with no zeros in the interval $(-\frac{1}{a}, \frac{1}{a})$ [47]. In this study, the roles of the parameters m_0, a and η on the vibrational resonance of a bistable oscillator are examined.

The general force equation for a PDM oscillator is

$$\begin{aligned} F(x, \dot{x};\ t) &= F(x;\ t) + R_{PDM}(x, \dot{x};\ t) \\ &= -\frac{dV(x)}{dx} + \phi, \end{aligned} \tag{4}$$

where the appearance of an overdot indicates differentiation with respect to time. Equation (4) include a modification to the Newton's equation for a system by including a reactive force $R_{PDM}(x, \dot{x}, t) = \frac{1}{2}\frac{dm(x)}{dx}$ which is quadratic in velocity [57]. The last term, $\phi = -\alpha\dot{x} + F_{ext}$, where α is the damping factor and $F_{ext} = f\cos\omega t + g\cos\Omega t$ is a dual-frequency external force comprising of a slow periodic input signal with frequency ω and a fast driving signal with frequency $\Omega(\Omega \gg \omega)$. The equation of motion (4) for a PDM system with inertial force $F(x;\ t) = m(x)\ddot{x}$ can thus be written as:

$$m(x)\ddot{x} + \frac{1}{2}\frac{dm(x)}{dx}\dot{x}^2 + \alpha\dot{x} + \frac{dV(x)}{dx} = F_{ext}. \tag{5}$$

Using Eqn (3), Eqn (5) can be written as a dissipative system with variable mass of the form:

$$\ddot{x} + b(x)\dot{x}^2 + c(x)\dot{x} + d(x) = h(x), \tag{6}$$

where

$$\begin{aligned} b(x) &= \frac{1}{2}\frac{m'(x)}{m(x)} = \frac{-a^2(\eta - 1)x}{(1 - a^2x^2)(1 - \eta a^2 x^2)}, \\ c(x) &= \frac{\alpha}{m(x)} = \frac{\alpha(1 - a^2x^2)}{m_0(1 - \eta a^2 x^2)}, \end{aligned} \tag{7}$$

$$
\begin{aligned}
d(x) &= \frac{1}{m(x)}\frac{dV(x)}{dx} \\
&= \omega_0^2 x + \omega_0^2 x^2 b(x) + \frac{\beta(1-a^2x^2)}{(1-\eta a^2x^2)m_0}x^3, \\
h(x) &= \frac{F_{ext}}{m(x)} = \frac{(1-a^2x^2)(f\cos\omega t + g\cos\Omega t)}{(1-\eta a^2x^2)m_0}.
\end{aligned}
$$

We can write the equation of motion (6) more explicitly by using equation (7) as:

$$
\begin{aligned}
\ddot{x} &- \frac{a^2(\eta-1)x}{(1-a^2x^2)(1-\eta a^2x^2)}\dot{x}^2 + \frac{\alpha(1-a^2x^2)}{m_0(1-\eta a^2x)}\dot{x} \\
&+ \omega_0^2 x - \omega_0^2 x^2 \frac{a^2(\eta-1)x}{(1-a^2x^2)(1-\eta a^2x^2)} \\
&+ \frac{\beta(1-a^2x^2)}{(1-\eta a^2x^2)m_0}x^3 \\
&= (f\cos\omega t + g\cos\Omega t)\frac{(1-a^2x^2)}{(1-\eta a^2x^2)m_0}.
\end{aligned} \tag{8}
$$

Equation (8) is the equation of motion for the PDM system modelling the ammonia molecule with Doubly-Singular mass function which is the focus of our analysis of VR in this paper.

3 Numerical Simulations

The response factor Q, also known as the response amplitude characterizes resonance. It provides an insight into how the parameters of a high-frequency signal coupled to a weakly driven nonlinear system leads to an amplified output. We computed numerically the response amplitude Q of the system at the frequency of the slow input signal from the Fourier spectrum of the output signal, because any periodic function can be approximately written as a sum of its Fourier components. Hence, we compute the response amplitude Q from the Fourier sine Q_s and cosine Q_c components which are given by

$$
\begin{aligned}
Q_s &= \frac{2}{nT}\int_0^{nT} x(t)\sin\omega t dt \\
Q_c &= \frac{2}{nT}\int_0^{nT} x(t)\cos\omega t dt,
\end{aligned} \tag{9}
$$

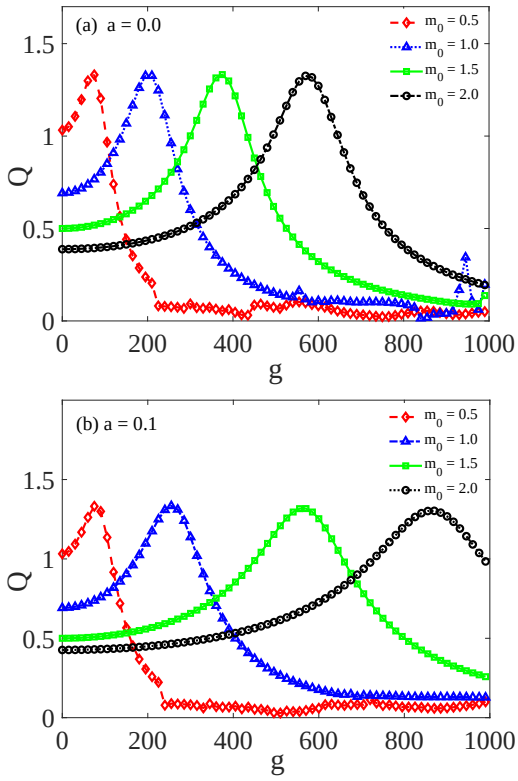

Fig. 1 Dependence of the response amplitude Q on HF signal amplitude g for four different values of constant fixed mass $m_0(0.5, 1.0, 1.5, 2.0)$ when (a) $a = 0.0$, and (b) $a = 0.1$. Fixed parameters are set as: $\alpha = 0.5$, $\beta = 1.0$, $\eta = -1$, $\omega = 1.5$, $\Omega = 10\omega$, $\omega_0^2 = 1$ and $f = 0.1$. The response amplitude Q computed by using the numerical solution of equation (8) in equation (10) are presented with lines and marker points of the same color.

so that the response amplitude Q and the phase shift Φ are then computed from Eqn. (9)

$$
Q = \frac{A}{F} = \frac{\sqrt{Q_s^2 + Q_c^2}}{F}, \tag{10}
$$

and

$$
\Phi = \tan^{-1}\left(\frac{Q_s}{Q_c}\right), \tag{11}
$$

respectively.

For the computation of the system's response given by equation (10), we solve equation (8) by first re-expressing it as a set of coupled first order autonomous differential equations of the form

$$
\dot{x} = y
$$

$$\dot{y} = \frac{a^2(\eta-1)x}{(1-a^2x^2)(1-\eta a^2x^2)}y^2 - \frac{\alpha(1-a^2x^2)}{m_0(1-\eta a^2x)}y - \omega_0^2 x + \omega_0^2 x^2 \frac{a^2(\eta-1)x}{(1-a^2x^2)(1-\eta a^2x^2)} - \frac{\beta(1-a^2x^2)}{(1-\eta a^2x^2)}x^3 + (f\cos\omega t + g\cos\Omega t)\frac{(1-a^2x^2)}{(1-\eta a^2x^2)m_0} \quad (12)$$

The response amplitude Q was computed from Eqn (12) for a range of values of the HF intensity parameter g and variable mass parameters (m_0, a, η).

We obtain the solution of Eqn (8) by integrating Eqn (12) over a time interval $T_s = nT$ using Fourth-Order Runge-Kutta scheme with step size of $\Delta t = 0.01$, where T $(= \frac{2\pi}{\omega})$ is the period of oscillation of the LF (ω) external signal, and n $(= 1, 2, 3, \dots)$ is the number of complete oscillations. The initial conditions $(x(0) = 0, y(0) = 1)$ were used, and the first $n = 100$ initial iterates were discarded as transient solutions.

Throughout our analysis, some system parameters are fixed as follows: $\alpha = 0.5$, $\beta = 1.0$, $\omega = 1.5$, $\omega_0^2 = 1$ and $f = 0.1$, while the parameters (g, Ω) of the high-frequency input signal and (m_0, a, η) of the variable mass were chosen within regimes that optimizes the occurrence of the resonance phenomenon.

4 RESULTS AND DISCUSSIONS

First, we examined the occurrence of VR for the PDM oscillator with constant mass by setting $a = 0$. Figure 1(a) shows the computed dependence of the response amplitude Q on the HF amplitude g for four values of fixed mass $m_0(= 0.5, 1.0, 1.5, 2.0)$. Clearly, for each fixed mass, the system exhibited distinct single resonance peak located at different values of HF amplitude. This resonance peaks were earlier observed for a Duffing oscillator with constant unitary mass. Indeed, the result in Figure 1(a) is consistent with results in earlier studies on Duffing oscillator with constant-unitary mass (when $m_0 = 1$) as presented by Rajasekar and Sanjuán [1] (see Figure 3.2). It can be observed that the increase in the value of the parameter m_0 increases the value of HF amplitude at which resonance occur (g_{VR}), which is marked by the point at which maximum response (Q_{max}) occur.

In Figure 1(b), the VR phenomenon observed for the system with constant mass is also found when the mass varies with position by setting $a = 0.1$. This is shown for the variation of Q against g for fixed values of constant mass ($m_0 = 0.5, m_0 = 1.0, m_0 = 1.5, m_0 = 2.0$). Again, single resonance peaks appears in each case. Comparatively, Figures 1(a) and 1(b) shows that the effect of increasing m_0 on g_{VR} becomes more pronounced when the mass variation is switched on. This implies that the parameters (m_0, a) of the variable mass have significant effect on the observed resonances. This effect can complement the role of the system parameters that are known to initiate resonance.

Next, we investigated the possibility of inducing resonance through the parameters of the variable mass in the presence of the high-frequency signal. To do this, we showed that VR can be induced by varying the reduced mass parameter m_0 in a PDM system with constant mass$(a = 0)$ and in a system with variable mass $(a = 0.05)$ presented in Figures 2(a) and 2(b), respectively through the dependence of response amplitude Q on the fixed mass m_0 for four values of HF amplitude g(=30,50,80,100). Remarkably, single resonance peaks reminiscent of the traditional bell-shaped response curves for the dependence of response amplitude on HF signal parameter as shown in Figure 1 were observed. This shows that VR can be induced by varying the constant fixed mass m_0.

The two possibilities of controlling and inducing VR by varying the constant fixed mass m_0 as highlighted above are also shown to be realizable with the separation coefficient a as shown in Figures 3(a) and 3(b), respectively. Figure 3(a) shows the dependence of Q on HF amplitude g for four values of the separation coefficient $a(= 0, 0.04, 0.05, 0.06)$ when $m_0 = 1$. Again, increasing a increases g_{VR} as observed for m_0. In addition, this implies that, under dual-frequency driving forces, the ammonia molecule can maximize the planar separation distance, coefficient a, to achieve maximal response of the ammonia molecule. The separation coefficient a can also be used to induce VR as shown in Figure 3(b), which depicts the dependence of Q on the separation coefficient a for four values of response amplitude g (30, 50, 80, 100) when $m_0 = 1$. Figure 3 shows

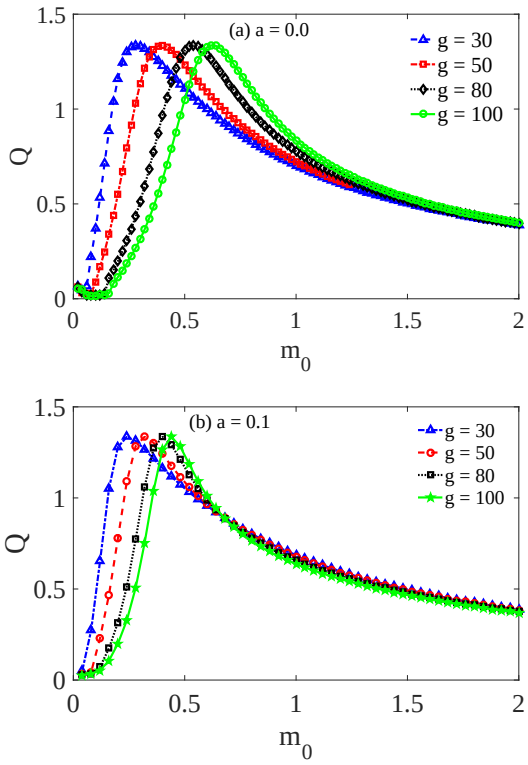

Fig. 2 Dependence of the response amplitude Q on rest mass m_0 for four different values of g ($g = 30, g = 50, g = 80, g = 100$) when (a) $a = 0.0$, and (b) where $a = 0.1$. Some parameters are fixed at: $\alpha = 0.5$, $\beta = 1.0$, $\eta = -1$, $\omega = 1.5$, $\Omega = 10\omega$, $\omega_0^2 = 1$ and $f = 0.1$. The response amplitude Q computed by using the numerical solution of equation (8) in equation (10) are presented with lines and marker points of the same color.

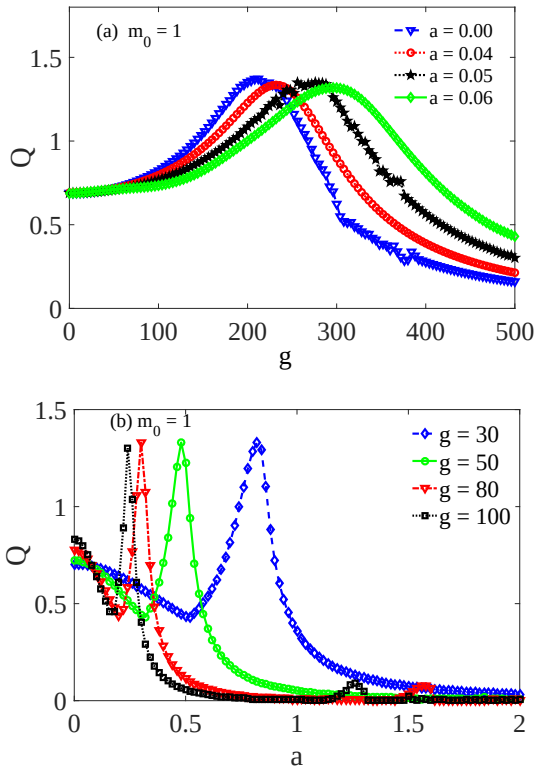

Fig. 3 Dependence of the response amplitude Q on (a) HF amplitude g for four different values separation coefficient $a(= 0, 0.04, 0.05, 0.06)$, and (b) separation coefficient a for four values of HF amplitude, $g = 30, g = 50, g = 80$, and $g = 100$. Other parameters are fixed as follows: $m_0 = 1$, $\alpha = 0.5$, $\beta = 1.0$, $\eta = -1$, $\omega = 1.5$, $\Omega = 10\omega$, $\omega_0^2 = 1$ and $f = 0.1$. The response amplitude Q computed by using the numerical solution of equation(8) in equation (10) are presented with lines and marker points of the same color.

that the VR can be achieved through the modulation of separation coefficient in the presence of the HF amplitude g. It is striking to note that, although the constant mass m_0, and the separation coefficient a for the spatial mass distribution function are effective in inducing VR, comparatively, it is apparently evident from the numerical simulation results that the variation of a gives rise to sharper resonance. In order to uncover the underlying mechanisms, we examined the associated bifurcation structure of the system with the parameters m_0 and a taken as bifurcation parameters. This is illustrated in Figures 4 and 5 where we compared the bifurcation structures using the parameters of Figure 2(b) and 3(b), respectively. In relation to Figure 2(b) for weak HF amplitude ($g \leq 30$), the bifurcation structure shown in Figure 4(a) reveals that, when the constant mass m_0 is varied a *period-one* attractor of the particle (marked with blue color) vibrates rapidly and asymptotically with decreasing velocity and attempts to reach a stable steady state as m_0 increase appreciably. On the contrary, when the mass function parameter a is varied the velocity of the *period-one* attractor (marked with red color) remains relatively stable over the range of a values computed as shown in Figure 4(a). As the values of the HF amplitude is increased (see Figure 4(b-d), the dynamics is consistent with the one shown in Figure 4(a), however, more periodic attractors emerges as the values of g increases. By plotting the bifurcation structure of the displacements x, it is found that, x rapidly increases for weaker values of g, typically, $g \leq 30$ (See Figure 5(a)). When the HF signal is sufficiently strong as shown in Figure 5(b-d), x first rapidly decreases, attains a

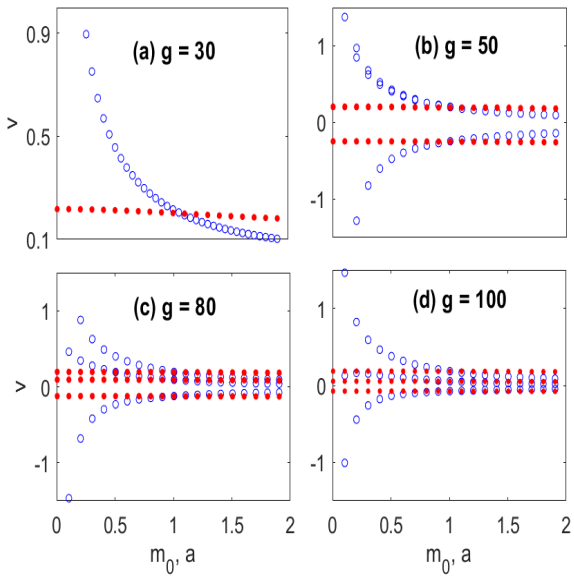

Fig. 4 The bifurcation diagram of the velocity, $v = \dot{x}$ as function of the separation coefficient a (red dots) superposed with the bifurcation diagram of the velocity as function of the rest mass m_0 (blue dots) for four different values of the HF amplitude g: (a) $g = 30$, (b) $g = 50$, (c) $g = 80$ and (d) $g = 100$. Other parameters are fixed as in Figure 2 and Figure 3.

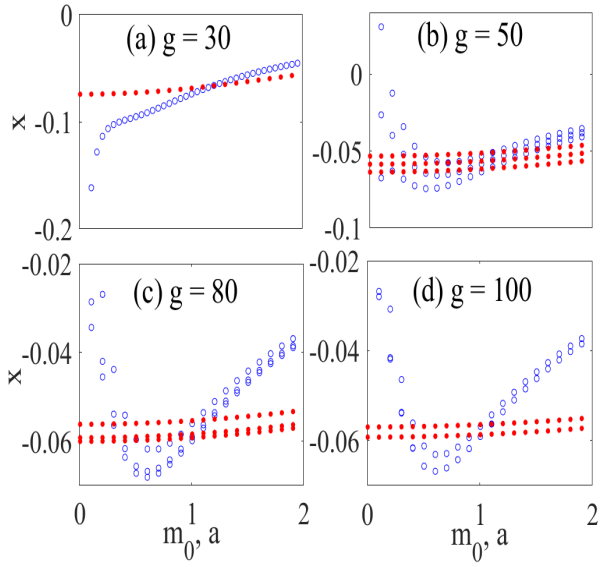

Fig. 5 The bifurcation diagram of the displacement, x as function of the separation coefficient a (red color) superposed with the bifurcation diagram of the displacement as function of the rest mass m_0 (blue dots) for two different values of the HF amplitude g: (a) $g = 30$, (b) $g = 50$, (c) $g = 80$ and (d) $g = 100$. Other parameters are fixed as in Figure 2 and Figure 3.

minimum value at $g = 0.6$ and thereafter increases rapidly. With a as the bifurcation parameter, however, the displacement is relatively stable over the range of a values. We conjecture that the rapid changes in the bifurcation structure with the variation of m_0 attempts to impede on the response to HF driving force, thereby accounting for the distinct response pattern observed in Figures 2 and 3.

Furthermore, we establish concretely VR-induced by PDM indices as shown in Figure 6, which illustrates the variation of Q with variable mass parameters (m_0 and a). In Figure 6(a), the single-peak resonance VR was induced by constant fixed mass m_0 and its modulation was achieved with four different values of the separation coefficient $a(0.0, 0.1, 0.2, 0.5)$ when $g = 50$. Next, we reversed the roles of the PDM parameters shown in Figure 6(a) in 6(b), so that resonance is induced by the separation coefficient a and its modulation was achieved with four values of constant mass m_0 $(0.5, 1.0, 1.5, 2.0)$ when $g = 30$. The implication of the plots in Figure 6 is that the two PDM parameters (m_0 and a) play complimentary roles in the induction of VR.

To complete the representation, Figure 6 is viewed in three-dimensions by scanning simultaneously the parameter space (m_0, a) for the occurrence of VR. The dependence of Q on the variable mass parameters m_0 and a is shown in Figure 7(a - d) for four fixed values of the HF amplitude $g = 30$, $g = 50$, $g = 80$ and $g = 100$. The VR phenomenon manifests in Figure 7 as ridge-shaped resonance peaks traversing along the planes of PDM parameters m_0 and a. Notably, the peaks are significantly pronounced for moderate values of g and appears for all values for which the parameter a and m_0 are defined. However, as g becomes appreciably larger, the peaks depresses progressively, occurring for all values for which the parameter m_0 is defined and in the neighbourhood of lower parameter values of a.

We remark that when the doubly-singular mass ratio $\eta = 0$, the position dependent mass distribution becomes a *regular mass function*, and the system (Equation (8)) is reduced to that considered by Roy-Layinde *et al.* [33]. Hence, we show that η also play a crucial role in the appearance of VR. In this regards, we analyzed VR by exploring the cooperation between HF amplitude g and dimensionless mass ratio η through a series

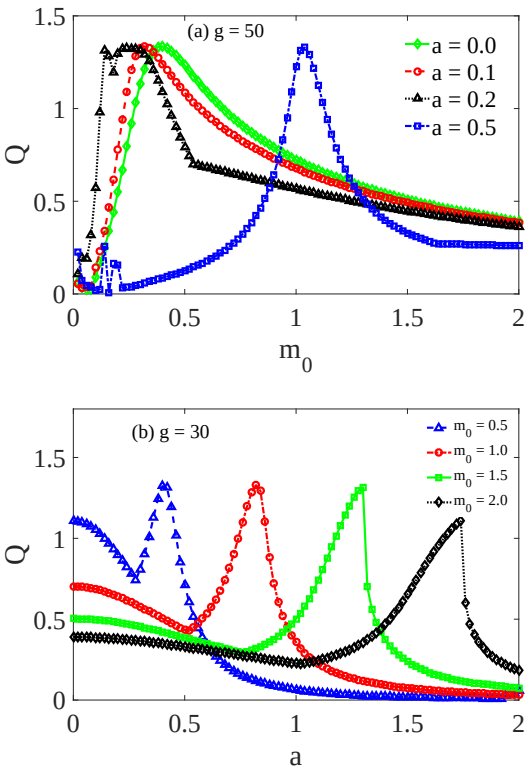

Fig. 6 Variation of response amplitude Q on (a) fixed mass m_0 for four different values of separation coefficient a $(0.00, 0.04, 0.05, 0.06)$ for HF amplitude $g = 50$, and (b) separation coefficient a for four values of m_0 $(0.5, 1.0, 1.5, 2.0)$ when $g = 30$. Other system parameters are fixed at: $\alpha = 0.5$, $\beta = 1.0$, $\eta = -1$, $\omega = 1.5$, $\Omega = 10\omega$, $\omega_0^2 = 1$ and $f = 0.1$. The response amplitude Q computed by using the numerical solution of equation (8) in equation (10) are presented with lines and marker points of the same color

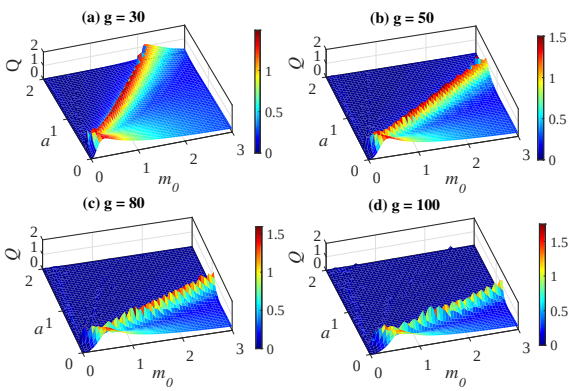

Fig. 7 The dependence of the response amplitude Q on separation coefficient a and the fixed mass m_0 for four values of the HF amplitude g: $(g = 30, g = 50, g = 80, g = 100)$ shown in (a-d), respectively. Other parameters are set as: $\alpha = 0.5$, $\beta = 1$, $\omega_0^2 = 1$ $\Omega = 15$, $\omega = 1.5$ and $f = 0.1$.

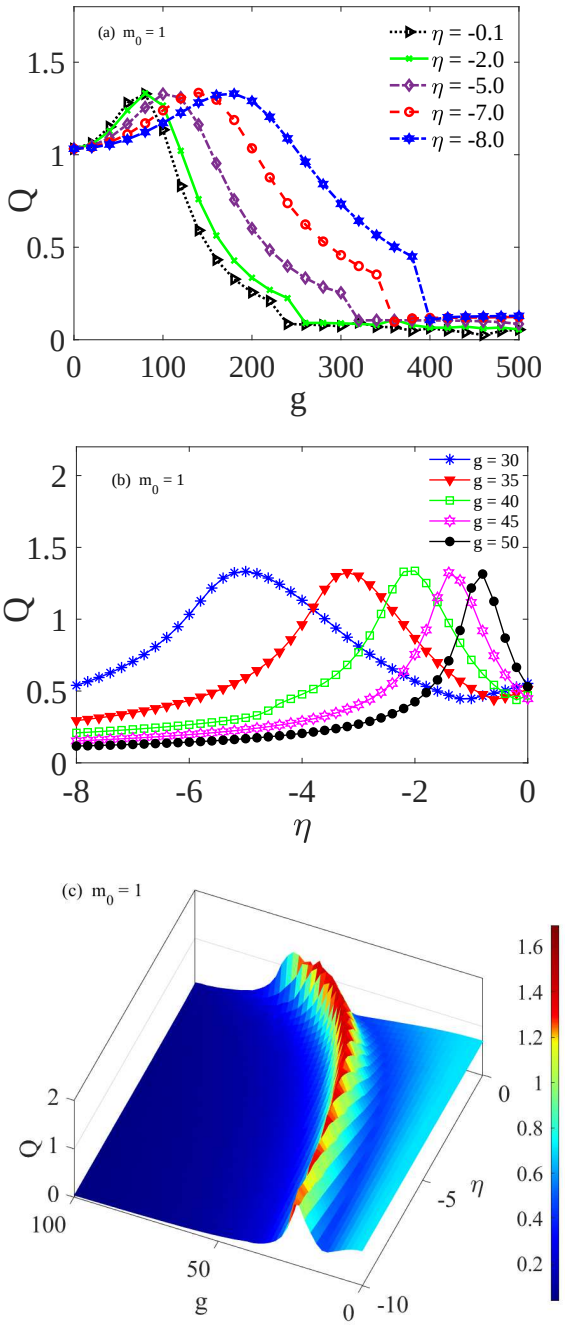

Fig. 8 Variation of response amplitude Q on (a) HF amplitude g for five different values η: $(\eta = -0.1, \eta = -2.0, \eta = -5.0, \eta = -7.0, \eta = -8.0)$ for the separation coefficient $a = 0.1$, (b) dimensionless parameter η for five values of HF amplitude, g: $g = 30, g = 35, g = 40, g = 45$, and $g = 50$ when $a = 0.5$, and (c) HF amplitude g and dimensionless parameter η in 3D when $a = 0.5$. Other system parameters are fixed at: $\alpha = 0.5$, $\beta = 1.0$, $\eta = -1$, $\omega = 1.5$, $\Omega = 10\omega$, $\omega_0^2 = 1$ and $f = 0.1$. The response amplitude Q computed by using the numerical solution of equation (8) in equation (10) are presented with lines and marker points of the same color.

of response curves determined for the dependence of response amplitude Q on amplitude g for five values of $\eta(\eta = -0.1, \eta = -2, \eta = -5, \eta = -7, \eta = -8)$ presented in Figure 8(a), and the dependence of Q on η for five values of HF amplitude $g(g = 30, g = 35, g = 40, g = 45, g = 50)$ as shown in Figure 8(b). In both instances, single-peak resonance curves amenable to varying system parameters are observed as depicted in Figure 8(a) and Figure 8(b) for different values of η and g, respectively. Figure 8(a) shows that η could be used to control VR phenomenon, specifically, the value of HF amplitude where resonance occur. Also, η induced VR in the presence of the HF signal (see Figure 8(b)). Evidently, η influences VR much like other system parameters a and m_0. The highlighted effects of η are elaborated by a 3D plot (shown in Figure 8(c)) depicting an interplay between the response amplitude Q, HF amplitude g and doubly-singular mass parameter η.

Finally, the impact of η on VR depicted by the response curves in Figure 2 is illustrated as a 3D plot showing the dependence of the response amplitude Q on the variable mass parameters m_0 and the HF amplitude g in Figure 9 for four values of the parameter η, namely, $\eta = -0.5$, $\eta = -1.0$, $\eta = -1.5$, $\eta = -2.0$. Notably, for $\eta = -0.5$, single-peak resonance appears as shown in Figure 9(a) for $\eta = -0.1$. However, significant qualitative changes occurs when η is decreased to $\eta = -1.0$ as depicted in Figure 9(b), with the system evolving from a single peak to double resonances when the HF amplitude is increased. This is an emergence of the so-called double-vibrational resonance (DVR) [3, 13, 58, 60] or bi-resonance phenomenon [61]. Single-peak ridge shaped resonance curves can be observed with moderate HF amplitudes g (typically, $g \leq 100$) which is consistent with Figure 2, while double resonance peaks appear at higher values of g. The transition from single peak to double resonance peaks at higher values of g becomes more prominent when η decreases as shown for $\eta = -1.5$ in 9(c) and $\eta = -2.0$ in 9(d), respectively. Indeed, the appearance of two peaks from a single peak as η decreases corresponds to period-doubling bifurcations of three coexisting resonating attractors, simultaneously emerging when the HF driving force acts on the system as shown in Figure 10. With the amplitude, g of the HF driving force chosen as the bifurcation parameter, it is evident that multiple period-doubling takes place as g increases - indicating the underlying mechanism accompanying the occurrence of DVR induced by position-dependent mass parameters. Roy-Layinde *et al.* [16] had reported double vibrational resonance in a driven plasma oscillator arising from the impact of nonlinear damping and associated with sequential appearance of symmetry-breaking bifurcations bifurcations sequence.

The occurrence of double vibrational is not limited to deterministically driven systems. There have been reports also of its occurrence in noise-driven systems, and in such systems, the phenomenon is referred to as double stochastic resonance (DSR) [62]. Very recently, the occurrence of DSR in different systems was classified and compared by Qiao *et al.* (See Table 1 [62]). Furthermore, a novel double inverse stochastic resonance (DISR) was found to occur at distinct presynaptic firing rates when both short-term depression (STD) and/or short-term facilitation (STF) mechanisms are taken into account with time delay in the Tsodyks-Markram model of dynamic synapses, while synapses with two minima are sandwiched by a barrier [63].

To complete the discussions, we highlight on some remarkable results on DVR arising from different dynamical conditions in contrast to the impact of PDM system with doubly-singular mass distribution function reported herein. For instance, in Jeyakumar *et al.* [3], double vibrational resonance peaks were found in the interval of the high-frequency amplitude values where the effective potential is single-well double-hump shape, however, with the resonant frequency ω_r oscillating. In a similar development, Jeyakumari *et al.* [13] reported double-resonance arises from the increased variation of the amplitude of the high-frequency driving force, with the two resonance peaks located nearly at equidistance point, while the maximum values of response, Q at these resonances are the same. However, the response curve was found to be asymmetrical about g_0, where g_0 is the value of the high-frequency signal at which the resonance frequency, ω_r is minimum.

In the overdamped double-well Duffing oscillator with fractional-order damping, Yang and Zhu [58], observed double-resonances with the fractional order parameter $\alpha > 1$. However, in the underdamped double-well potential system, both

ordinary damping and fractional damping are capable of inducing double-resonances, in addition to the occurrence of one or two kind of single-resonance.

Very recently, it was shown that different forms of electromagnetic induction in a high-frequency driven single excitable FitzHugh–Nagumo (FHN) neuron and the FHN neuron coupled to feed-forward feedback network (FFN) system, respectively can induce double resonances, referred to as bi-resonance as reported by Ge *et al.* [61]. Calim *et al.* [20] also detected the emergence of DVR in a dual-frequency driven neuron interacting with astrocytes - a special kind of glial cells. DVR in this interacting neuron-astrocyte system, was found to be strongly dependent on the neuron–astrocyte interaction strength as well as the gliotransmitter production and degradation rates; and occurs via a slow, long-time variation in neuronal excitability that can be influenced significantly by the oscillation of astrocytic calcium when astrocytic Ca^{2+} dynamics are appropriately adjusted. Furthermore, abundances of double resonances, referred to as *reentrance-like vibrational resonance* was recently observed in an enzymatic-substrate reaction mode in which a sequence of switches from *single peak* $\rightarrow$ *double peaks* $\rightarrow$ *single peak* takes place when the fractional order time-derivatives of an enzymatic-substrate reaction model as well as the potential parameters are varied [60]. Contrarily, only a switch from *single peak* $\rightarrow$ *double peaks* takes place when the system's nonlinear parameter tuned.

To sum up, we emphasize that all the reports of DVR in Refs. [3, 13, 20, 58, 60, 61] and in some other literature where they exist are, to the best of our knowledge, limited to systems without mass variation - in either position, velocity or time. In particular, the coefficient of nonlinearity of the mass function defined as the doubly-singular mass ratio η, plays a key role in the induction of DVR in the present work suggesting that the type of the mass function can determine the outcome of a system's response to dual-frequency driving forces.

5 Conclusions

In this paper, we have examined vibrational resonance in a dual-frequency driven PDM oscillator describing the inversion of NH_3 molecule whose

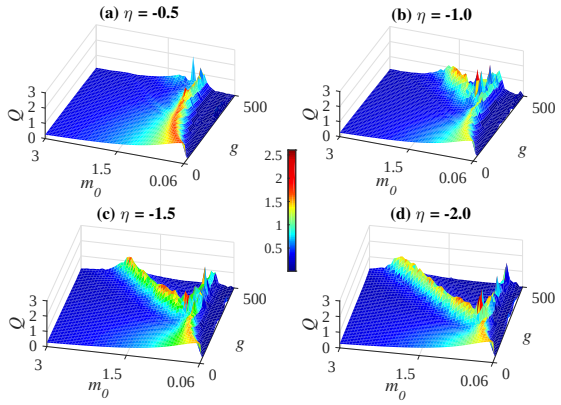

Fig. 9 The dependence of the response amplitude Q on fixed mass m_0 and HF amplitude g for four values of η: $(\eta = -0.5, \eta = -1.0, \eta = -1.5, \eta = -2.0)$ shown in (a-d), respectively. Other parameters are set as: $\alpha = 0.5$, $\beta = 1$, $\omega_0^2 = 1$, $\Omega = 15$, $\omega = 1.5$ and $f = 0.1$.

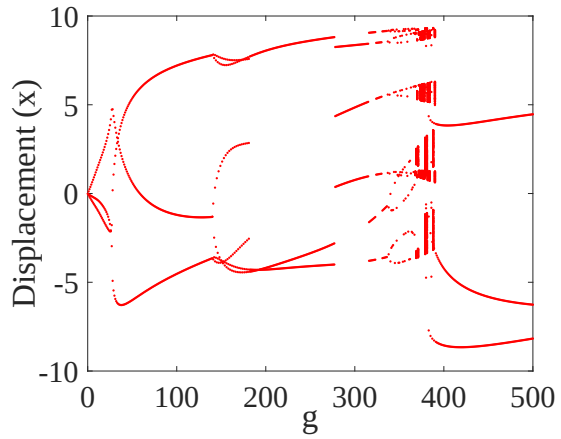

Fig. 10 The bifurcation diagram of the velocity, $\dot{x}$ as function of the HF amplitude, g for $\eta = -2.0$), respectively. Other parameters are set as: $\alpha = 0.5$, $\beta = 1$, $\omega_0^2 = 1$, $\Omega = 15$, $\omega = 1.5$, $m_0 = 0.06$ and $f = 0.1$.

mass is modeled as a doubly singular distribution with three parameters, a constant mass amplitude m_0, mass ratio η and separation coefficient a. We analyzed the influence of the constant mass m_0 on VR in the oscillator and showed that all the mass parameters (m_0, a and η) play vital roles in induction and control of VR. In addition to the appearance of single peak VR curves realized by varying the mass parameters a, m_0 and η in the presence of the HF signal, we showed that a good choice of doubly-singular mass ratio η, could drive the system to also undergo double resonance vibration state. This intriguing result, which was

not found in our recent paper on VR in PDM oscillators [33] also differs in its underlying mechanism from our previous paper on VR in a plasma oscillator [16] and other previous works. We conjecture that a wide range of PDM functions (with and without singularity) such as the symmetric soliton mass function [64], reflecting asymmetric mass function [65], asymmetric singular mass function [66], infinite mass function [67], mass function for semiconductor heterostructures [68], random mass function [69], etc. could lead to the appearance of novel vibrational and stochastic resonance phenomena when the system is driven by dual-frequency forces. Our findings provide a novel direction for understanding vibrational modes and spectroscopy of a wide range of heterogeneous structures. Moreover, the investigation of VR in network of PDM oscillators, such as found in the network of neurons [70, 71] could shed some lights on the separation of mixture of massive particles of different sizes by compelling them to occupy different equilibrium positions [20, 72, 73]. This is a possible direction for future work.

Acknowledgements

The authors are immensely grateful to the reviewers for their constructive comments and suggestions which were useful in improving the quality of the paper.

References

[1] S. Rajasekar, M. A. F. Sanjuán, Nonlinear Resonances, Springer Series in Synergetics, Springer, Switzerland, 2016.

[2] U. E. Vincent, P. V. McClintock, I. A. Khovanov, S. Rajasekar, Vibrational and stochastic resonances in driven nonlinear systems (2021).

[3] S. Jeyakumari, V. Chinnathambi, S. Rajasekar, M. A. F. Sanjuan, Single and multiple vibrational resonance in a quintic oscillator with monostable potentials, Phys. Rev. E 80 (4) (2009) 046608.

[4] M. Gitterman, Bistable oscillator driven by two periodic fields, J. Phys. A: Math. & Gen. 34 (24) (2001) L355.

[5] C. Yao, M. Zhan, Signal transmission by vibrational resonance in one-way coupled bistable systems, Phys. Rev. E 81 (6) (2010) 061129.

[6] V. N. Chizhevsky, G. Giacomelli, Experimental and theoretical study of vibrational resonance in a bistable system with asymmetry, Phys. Rev. E 73 (2) (2006) 022103.

[7] J. H. Yang, X. B. Liu, Controlling vibrational resonance in a multistable system by time delay, Chaos 20 (3) (2010) 033124.

[8] S. Rajasekar, K. Abirami, M. A. F. Sanjuán, Novel vibrational resonance in multistable systems, Chaos 21 (3) (2011) 033106.

[9] V. N. Chizhevsky, Experimental evidence of vibrational resonance in a multistable system, Phys. Rev. E 89 (2014) 062914.

[10] T. O. Roy-Layinde, J. A. Laoye, O. O. Popoola, U. E. Vincent, P. V. E. McClintock, Vibrational resonance in an inhomogeneous medium with periodic dissipation, Phys. Rev. E 96 (2017) 032209.

[11] U. E. Vincent, T. O. Roy-Layinde, P. O. Adesina, O. O. Popoola, P. V. E. McClintock, Vibrational resonance in an oscillator with an asymmetrical deformable potential, Phys. Rev. E 98 (2018) 062203.

[12] S. Jeyakumari, V. Chinnathambi, S. Rajasekar, M. A. F. Sanjuán, Vibrational resonance in an asymmetric Duffing oscillator, Inter. J. Bifurc. & Chaos 21 (01) (2011) 275–286.

[13] S. Jeyakumari, V. Chinnathambi, S. Rajasekar, M. A. F. Sanjuan, Analysis of vibrational resonance in a quintic oscillator, Chaos 19 (4) (2009) 043128.

[14] Y. Pan, F. Duan, F. Chapeau-Blondeau, L. Xu, D. Abbott, Study of vibrational resonance in nonlinear signal processing, Phil. Trans. Roy. Soc. A 379 (2192) (2021) 20200235.

[15] S. Morfu, B. Usama, P. Marquié, On some applications of vibrational resonance on noisy image perception: the role of the perturbation parameters, Phil. Trans. Roy. Soc. A 379 (2198) (2021) 20200240.

[16] T. O. Roy-Layinde, J. A. Laoye, O. O. Popoola, U. E. Vincent, Analysis of vibrational resonance in bi-harmonically driven plasma, Chaos 26 (9) (2016) 093117.

[17] K. A. Omoteso, T. O. Roy-Layinde, J. A. Laoye, U. E. Vincent, P. V. E. McClintock, Acoustic vibrational resonance in a Rayleigh-Plesset bubble oscillator, Ultrason. Sonochem. 70 (2021) 105346.

[18] V. Chizhevsky, Amplification of optical signals in a bistable vertical-cavity surface-emitting laser by vibrational resonance, Phil. Trans. Roy. Soc. A 379 (2192) (2021) 20200241.

[19] H. Yu, J. Wang, C. Liu, B. Deng, X. Wei, Vibrational resonance in excitable neuronal systems, Chaos 21 (4) (2011) 043101.

[20] A. Calim, T. Palabas, M. Uzuntarla, Stochastic and vibrational resonance in complex networks of neurons, Phil. Trans. Roy. Soc. A 379 (2198) (2021) 20200236.

[21] K. S. Oyeleke, O. I. Olusola, U. E. Vincent, D. Ghosh, P. V. E. McClintock, Parametric vibrational resonance in a gyroscope driven by dual-frequency forces, Phys. Lett. A 387 (2021) 127040.

[22] P. K. Sahoo, S. Chatterjee, High-frequency vibrational control of principal parametric resonance of a nonlinear cantilever beam: Theory and experiment, J. Sound & Vibr. 505 (2021) 116138.

[23] O. I. Olusola, O. P. Shomotun, U. E. Vincent, P. V. E. McClintock, Quantum vibrational resonance in a dual-frequency-driven Tietz-Hua quantum well, Phys. Rev. E 101 (5) (2020) 052216.

[24] S. Paul, D. Shankar Ray, Vibrational resonance in a driven two-level quantum system, linear and nonlinear response, Phil. Trans. Roy. Soc. A 379 (2192) (2021) 20200231.

[25] H. Irschik, A. K. Belyaev, Dynamics of mechanical systems with variable mass, Vol. 557, Springer, 2014.

[26] A. Nanjangud, F. O. Eke, Angular momentum of free variable mass systems is partially conserved, Aerospace Sc. & Tech. 79 (2018) 1–4.

[27] J. Awrejcewicz, Dynamics of systems of variable mass, in: Classical Mechanics, Springer, 2012, pp. 341–357.

[28] C. P. Pesce, L. Casetta, Systems with mass explicitly dependent on position, in: Dynamics of mechanical systems with variable mass, Springer, 2014, pp. 51–106.

[29] A. Johansen, M.-M. Mac Low, P. Lacerda, M. Bizzarro, Growth of asteroids, planetary embryos, and kuiper belt objects by chondrule accretion, Science Advances 1 (3) (2015) e1500109.

[30] W. T. Thomson, Equations of motion for the variable mass system., AIAA Journal 4 (4) (1966) 766–768.

[31] F. O. Eke, T. C. Mao, On the dynamics of variable mass systems, Int. J. Mech. Eng. Educ. 30 (2) (2002) 123–137.

[32] M. Jiang, J. Wu, S. Liu, The influence of slowly varying mass on severity of dynamics nonlinearity of bearing-rotor systems with pedestal looseness, Shock & Vibr. 2018 (2018) 3795848.

[33] T. O. Roy-Layinde, U. E. Vincent, S. A. Abolade, O. O. Popoola, J. A. Laoye, P. V. E. McClintock, Vibrational resonances in driven oscillators with position-dependent mass, Phil. Trans. Roy. Soc. A 379 (2192) (2021) 20200227.

[34] B. Bagchi, S. Das, S. Ghosh, S. Poria, Nonlinear dynamics of a position-dependent mass-driven Duffing-type oscillator, J. Phys. A: Math. & Theor. 46 (3) (2012) 032001.

[35] L. A. Hinvi, A. A. Koukpémèdji, V. A. Monwanou, C. H. Miwadinou, V. Kamdoum Tamba, J. B. Chabi Orou, Resonance, chaos and coexistence of attractors in a position dependent mass-driven Duffing-type oscillator, J. Korean Phys. Soc. 79 (2021) 755–771.

[36] R. Khordad, Effect of position-dependent effective mass on linear and nonlinear optical properties in a quantum dot, Indian J. Phys. 86 (6) (2012) 513–519.

[37] O. von Roos, Position-dependent effective masses in semiconductor theory, Phys. Rev. B 27 (12) (1983) 7547.

[38] M. R. Geller, W. Kohn, Quantum mechanics of electrons in crystals with graded composition, Phys. Rev. Lett. 70 (20) (1993) 3103.

[39] F. Zhao, X. Liang, S. Ban, Influence of the spatially dependent effective mass on bound polarons in finite parabolic quantum wells, Eur. Phys. J. B 33 (1) (2003) 3–8.

[40] F. A. De Saavedra, J. Boronat, A. Polls, A. Fabrocini, Effective mass of one ^{4}He atom in liquid ^{3}He, Phys. Rev. B 50 (6) (1994) 4248.

[41] B. G. da Costa, E. P. Borges, A position-dependent mass harmonic oscillator and deformed space, J. Math. Phys. 59 (4) (2018) 042101.

[42] J. Yu, S.-H. Dong, G.-H. Sun, Series solutions of the Schrödinger equation with position-dependent mass for the Morse potential, Phys. Lett. A 322 (5-6) (2004) 290–297.

[43] H. A. Bethe, Possible explanation of the solar-neutrino puzzle, Phys. Rev. Lett. 56 (12) (1986) 1305.

[44] M. Barranco, M. Pi, S. M. Gatica, E. S. Hernández, J. Navarro, Structure and energetics of mixed ^{4}He-^{3}He drops, Phys. Rev. B 56 (14) (1997) 8997.

[45] R. A. El-Nabulsi, Dynamics of position-dependent mass particle in crystal lattices microstructures, Physica E 127 (2021) 114525.

[46] P. Ring, P. Schuck, The nuclear many-body problem (1980).

[47] S. Cruz Y Cruz, O. Rosas-Ortiz, Dynamical equations, invariants and spectrum generating algebras of mechanical systems with position-dependent mass, SIGMA. Symmetry, Integrability and Geometry: Methods and Applications 9 (2013) 004–21.

[48] A. G. Schmidt, Wave-packet revival for the schrödinger equation with position-dependent mass, Phys. Lett. A 353 (6) (2006) 459–462.

[49] N. Aquino, G. Campoy, H. Yee-Madeira, The inversion potential for NH_3 using a DFT approach, Chem. Phys. Lett. 296 (1-2) (1998) 111–116.

[50] R. A. El-Nabulsi, Position-dependent mass fractal Schrödinger equation from fractal anisotropy and product-like fractal measure and its implications in quantum dots and nanocrystals, Optical and Quantum Elec. 53 (9) (2021) 1–19.

[51] A. Sitnitsky, Exactly solvable Schrödinger equation with double-well potential for hydrogen bond, Chem. Phys. Lett. 676 (2017) 169–173.

[52] A. Sitnitsky, Analytic description of inversion vibrational mode for ammonia molecule, Vibrational Spectroscopy 93 (2017) 36–41.

[53] C. A. Downing, On a solution of the Schrödinger equation with a hyperbolic double-well potential, J. & Math. Phys. 54 (7) (2013) 072101.

[54] R. R. Hartmann, Bound states in a hyperbolic asymmetric double-well, J. Math. Phys. 55 (1) (2014) 012105.

[55] W. T. King, Quadratic potential function for ammonia, J. Chem. Phys. 36 (1) (1962) 165–170.

[56] J. D. Swalen, J. A. Ibers, Potential function for the inversion of ammonia, J. Chem. Phys. 36 (7) (1962) 1914–1918.

[57] O. Mustafa, Comment on 'nonlinear dynamics of a position-dependent mass-driven duffing-type oscillator', J. Phys. A: Math. & Theor. 46 (36) (2013) 368001.

[58] J. H. Yang, H. Zhu, Vibrational resonance in duffing systems with fractional-order damping, Chaos 22 (1) (2012) 013112.

[59] A. Calim, A. Longtin, M. Uzuntarla, Vibrational resonance in a neuron-astrocyte coupled model, Phil. Trans. Roy. Soc. A 379 (2198) (2021) 20200267.

[60] P. Fu, C.-J. Wang, K.-L. Yang, X.-B. Li, B. Yu, Reentrance-like vibrational resonance in a fractional-order birhythmic biological system, Chaos, Solitons & Fractals 155 (2022) 111649.

[61] M. Ge, L. Lu, Y. Xu, R. Mamatimin, Q. Pei, Y. Jia, Vibrational mono-/bi-resonance and wave propagation in fitzhugh–nagumo neural systems under electromagnetic induction, Chaos, Solitons & Fractals 133 (2020) 109645.

[62] Z. Qiao, J. Liu, X. Ma, J. Liu, Double stochastic resonance induced by varying potential-well depth and width, Journal of the Franklin Institute 358 (3) (2021) 2194–2211.

[63] M. Uzuntarla, J. J. Torres, P. So, M. Ozer, E. Barreto, Double inverse stochastic resonance with dynamic synapses, Phys. Rev. E 95 (2017) 012404.

[64] G. Yañez-Navarro, G.-H. Sun, T. Dytrych, K. D. Launey, S.-H. Dong, J. P. Draayer, Quantum information entropies for position-dependent mass schrödinger problem, Annals of Physics 348 (2014) 153–160.

[65] R. N. Costa Filho, M. P. Almeida, G. A. Farias, J. S. Andrade, Displacement operator for quantum systems with position-dependent mass, Phys. Rev. A 84 (2011) 050102.

[66] S.-H. DONG, J. J. PEÑA, C. PACHECO-GARCÍA, J. GARCÍA-RAVELO, Algebraic approach to the position-dependent mass schrödinger equation for a singular oscillator, Modern Physics Letters A 22 (14) (2007) 1039–1045.

[67] J. Asad, P. Mallick, M. Samei, B. Rath, P. Mohapatra, H. Shanak, R. Jarrar, Asymmetric variation of a finite mass harmonic like oscillator, Results in Physics 19 (2020) 103335.

[68] R. A. El-Nabulsi, A new approach to the schrodinger equation with position-dependent mass and its implications in quantum dots and semiconductors, J. Phys. Chem. Solids 140 (2020) 109384.

[69] M. Gitterman, Stochastic oscillator with random mass: New type of brownian motion, Physica A 395 (2014) 11–21.

[70] M. Uzuntarla, E. Yilmaz, A. Wagemakers, M. Ozer, Vibrational resonance in a heterogeneous scale free network of neurons, Comm. Nonl. Sci. Numer. Simulat. 22 (1) (2015) 367–374.

[71] S. N. Agaoglu, A. Calim, P. Hövel, M. Ozer, M. Uzuntarla, Vibrational resonance in a scale-free network with different coupling schemes, Neurocomputing 325 (2019) 59–66.

[72] J. Zhang, S. Yan, R. Sluyter, W. Li, G. Alici, N.-T. Nguyen, Inertial particle separation by differential equilibrium positions in a symmetrical serpentine micro-channel, Scientific Reports 4 (1) (2014) 4527.

[73] J. Palumbo, M. Navi, S. S. H. Tsai, J. K. Spelt, M. Papini, Inertial particle separation in helical channels: A calibrated numerical analysis, AIP Advances 10 (12) (2020) 125101.